MRS Advances © 2019 Materials Research Society
DOI: 10.1557/adv.2019.260

Magnetic Properties of Proton Irradiated $Mn_3Si_2Te_6$ van der Waals Single Crystals

L. M. Martinez[1], C. L. Saiz[1], A. Cosio[1], R. Olmos[1], H. Iturriaga[1], L. Shao[2], S. R. Singamaneni[1]

[1]*Department of Physics, The University of Texas at El Paso, El Paso, TX 79968, USA*

[2]*Department of Nuclear Engineering, Texas A&M University, College Station, TX 77845, USA*

ABSTRACT

The bulk van der Waals crystal $Mn_3Si_2Te_6$ (MST) has been irradiated with a proton beam of 2 MeV at a fluence of 1×10^{18} H^+ cm^{-2}. The temperature dependent magnetization measurements show a drastic decrease in the magnetization of 49.2% in the H//c direction observed in ferrimagnetic state. This decrease in magnetization is also reflected in the isothermal magnetization curves. No significant change in the ferrimagnetic transition temperature (75 K) was reflected after irradiation. Electron paramagnetic resonance (EPR) spectroscopy shows no magnetically active defects present after irradiation. Here, experimental findings gathered from MST bulk crystals via magnetic measurements, magnetocaloric effect, and heat capacity are discussed.

INTRODUCTION

Research in graphene began a revolution that has led to a profound interest in two-dimensional (2D) materials [1–3]. Although graphene and other 2D materials, such as transition metal dichalcogenides (TMDs), have exhibited attractive mechanical and optical properties, the possibility of introducing magnetism into these materials has received limited interest until now [4]. A recent surge in the interest for the layered van der Waals (vdW) crystals has opened doors for many researchers to take these materials to the 2D limit [1,2]. Various studies have shown that the magnetism in these vdW materials can be retained down to the monolayer limit [5–7]. An example of this phenomena is CrI_3, a layer dependent vdW material that exhibits ferromagnetic behaviour in its monolayer and bulk form, yet exhibits antiferromagnetic behaviour in its

bilayer form [5]. The ability to manipulate the magnetism in these materials by tuning the number of layers is highly desirable, especially when ferromagnetic ordering can be achieved at higher temperatures. For instance, bulk $CrSiTe_3$ (CST) exhibits ferromagnetic ordering at T = 32 K, but can be manipulated to exhibit this ordering at about 80 K by simple mechanical exfoliation down to the monolayer [8]. Although this class of materials may produce ferromagnetic behaviour at a higher temperature, it is still drastically lower than the desired temperature (300 K) for practical applications [3]. In order to reach the desired room temperature ferromagnetism, a better understanding of the properties of these vdW crystals is needed. Of particular interest is the vdW crystal $Mn_3Si_2Te_6$ (MST), a less studied analogue of CST that displays ferrimagnetic behaviour in the bulk form and has a transition temperature of 75 K with magnetic moments lying along the *ab* plane [9,10].

As outlined above, the magnetic behaviour of these materials can be tuned by varying the number of layers through mechanical exfoliation. However, changing their magnetic properties through ion irradiation [11–13] is a versatile and promising method. Previous reports have shown that highly oriented pyrolytic graphite exhibited ferromagnetic ordering with a Curie temperature (T_C) above room temperature after proton irradiation [14]. Lee *et al*. used EPR to reveal the origin of the ferromagnetism found in graphite after proton irradiation through the controlled introduction of defects which contain unpaired electron spins [15]. Another report on MoS_2, which is diamagnetic in nature, showed ferro or ferri-magnetic ordering with T_C = 895 K after being irradiated with a 2 MeV proton beam [16]. In addition, electron irradiation has also been used to induce ferromagnetism and change the easy axis (depending on the fluence of the irradiation) [12]. The possibility of inducing ferromagnetic behaviour in these non-magnetic materials through irradiation is due to the controlled introduction of lattice distortions, structural disorder or other defects [14,16,17].

As these vdW materials keep receiving attention and their properties are able to be enhanced, greater application opportunities open up. At some point in time, vdW materials are projected to be used in nano-electronics and memory storage devices [18,19]. As the popularity of these devices increase, they may even be used in near-Earth orbit applications. Such applications will encounter proton irradiation in space [20], so it is imperative that the effect of irradiation on bulk systems is well understood.

In this paper, the magnetic properties of MST single crystal before and after proton irradiation with a 2 MeV beam at a fluence of 1×10^{18} cm^{-2} is reported. A remarkable decrease (49.4% for H//*c*) in magnetization was observed in the temperature dependent magnetization of MST in ferrimagnetic state. However, no significant change in the transition temperature upon proton irradiation is observed from the temperature dependent magnetization, magneto-caloric effect (MCE) data, and heat capacity measurements. EPR spectra reveals Mn^{2+} paramagnetic signals from both pristine and irradiated crystals with no additional magnetically active defects present after irradiation.

EXPERIMENTAL DETAILS

MST single crystals were grown by melting of stoichiometric mixture of pure elements, as described in our previous reports [10]. Approximate crystal size for single crystals is 3 mm. Crystals were irradiated with a 2 MeV proton beam with a fluence of 1×10^{18} cm^{-2}. The proton beam spot size is 6mm x 6mm, with a beam current of ~1 μA. The beam is filtered with multiple magnet bending devices to remove carbon contamination [21,22]. During the irradiation process, the vacuum maintains a pressure of 6×10^{-8} Torr or lower. Liquid nitrogen trapping is applied during irradiation in order to improve the vacuum. The projected range of 2 MeV H^+ ions is about 30 microns. The

damage profile has a relative flat distribution from the surface up to ~30 microns. The magnetic properties of the single crystals were measured using a Quantum Design Cryogen-free VersaLab^{TM}. The VersaLab's vibrating sample magnetometer (VSM) setup is used to conduct measurements at a temperature range of 50-400 K, with an applied magnetic field of ± 3 T. In-plane (H//*c*) and out-of-plane (H//*ab)* measurements were performed using a standard VSM coil set.

RESULTS AND DISCUSSION

The temperature dependent magnetization for pristine and irradiated MST single crystals is shown in Figure 1(a, b). The transition temperature found for the pristine and irradiated crystals was ~ 73 K, which is in close agreement to the reported value of ~ 75 K [9,10]. In the present study, the temperature dependent magnetization obtained on the pristine MST crystal in the ferrimagnetic phase (at 50 K) is consistent with that of a previous study conducted on the same compound [9], where the magnetization is ~ 10 times greater when measured in the H//*ab* than that of when measured in the H//*c*. In Figure 1(a), where the M(T) measurement is performed with the field applied parallel to the *ab*-plane, the magnetization shows a decrease from 14.2 to 12.9 emu/g, after irradiation. Most remarkably, when the M(T) curves are measured with the field applied parallel to the c-axis (Figure 1(b)), we noticed a dramatic decrease (49.2%) in the magnetization from 1.33 to 0.68 emu/g in the ferrimagnetic region. An estimate of the transition temperature (~ 73 K) was found by taking the d*M*/dT (not shown).

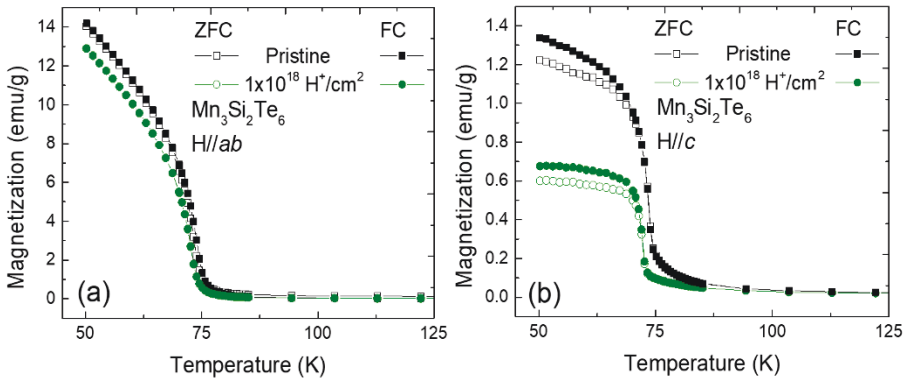

Figure 1. Magnetization as a function of temperature performed with the field applied perpendicular (a) and parallel (b) to the c axis. In each part the Zero-Field-Cooling (ZFC) curve and Field-Cooling (FC) curve (performed by cooling the sample down with H = 1 kOe and then changing the measuring field to 500 Oe) are shown.

The isothermal magnetization for the pristine and irradiated MST crystals shown in Figure 2(a, b) were performed with the field parallel and perpendicular with the crystallographic c-axis. As presented in Figure 2(a), irradiation caused a decrease in saturation magnetization (M_S) (from 0.96 to 0.86 μ_B/Mn), consistent with the decrease found in our M(T) data (see Fig. 1). A decrease (from 0.55 to 0.44 μ_B/Mn) in the saturation magnetization was also observed in Figure 2(b) after irradiation. It should be noted that our M_S is a fraction (17%) of the expected spin-only moment (5.6 μ_B/Mn) due

to Mn^{2+} ions present in MST. This detail was noted previously by May *et al.* and was attributed to uncompensated Mn^{2+} local moments in the ordered state [9]. No remnant magnetization is observed for both systems, which is a good indication of the high crystallinity for MST even after irradiation [9,10].

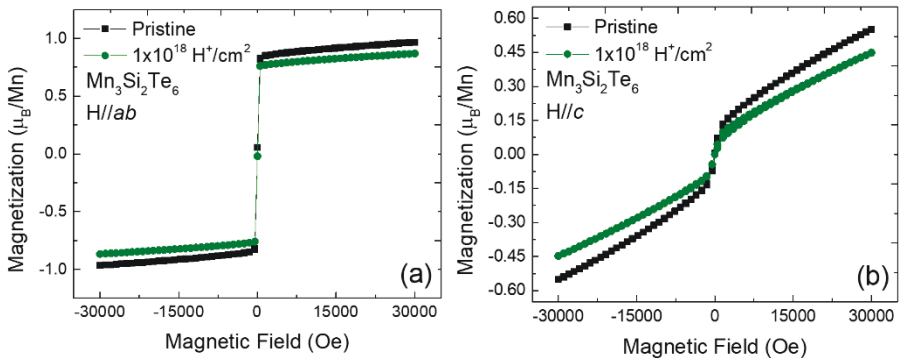

Figure 2. The isothermal magnetization for MST (pristine and irradiated) taken at 50 K and performed with H//*ab* (a) and H//*c* (b) directions.

The magnetic entropy change, seen in Figure 3(a, b), was obtained using similar methods applied in Ref. [8]. This allows the temperature dependent $-\Delta S_M$ curves at different fields to be obtained. A broad peak is observed at the transition temperature of MST with asymmetry present along the sides of the peak, similarly observed by Liu *et al.* [10]. The peaks for both pristine and irradiated crystals are found at ~ 74 K, in agreement with the estimated transition found through the dM/dT curves. Additionally, the maximum entropy value ($-\Delta S_M$) was found to be ~ 1.6 J kg^{-1} K^{-1} in both crystals, thus signifying that no additional disorder had been introduced upon proton irradiation. Heat capacity measurements were also performed for pristine and irradiated MST crystals, seen in Figure 4. A relatively broad peak was observed at ~73 K, consistent with the transition temperature estimated from magnetization and MCE data.

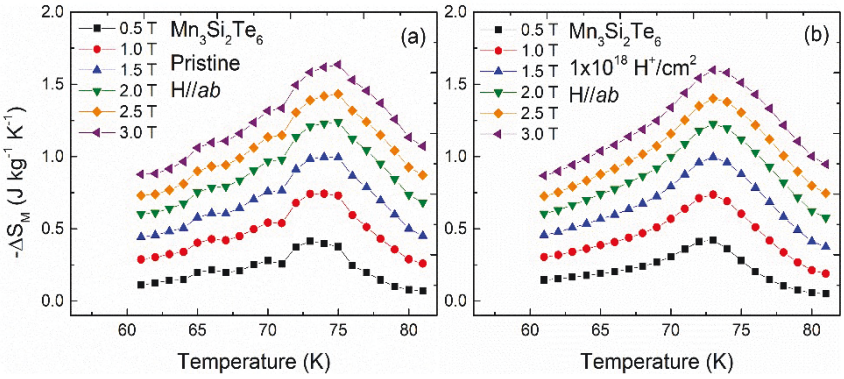

Figure 3. The temperature dependence of magnetic anisotropy obtained from MST crystal before and after proton irradiation measured on (a) pristine and (b) irradiated samples.

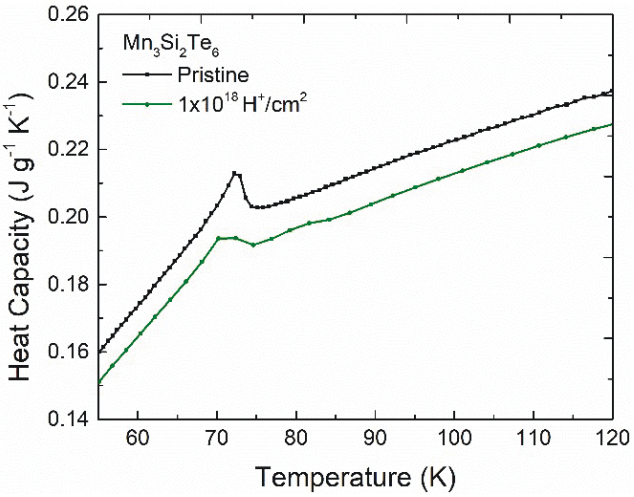

Figure 4. The temperature dependence of heat capacity for pristine and irradiated MST crystal. In both the curves the peak at around 73 K shows the ferrimagnetic phase transition.

EPR spectroscopy is a powerful technique to probe the atomic paramagnetic sites and defects present in materials. Figure 5 shows the X-band (9.43 GHz) EPR spectra for pristine and irradiated MST collected at 50 K in the ferrimagnetic phase. Upon closer inspection, the spectra show two overlapped signals. We have deconvoluted these signals with computer generated fits using Lorentzian and Dysonian line shapes [23–25]. A sharp Lorentzian line-shape was observed from both the pristine and irradiated MST samples. The g-value corresponding to this Lorentzian signal was found to be 1.9956 in both the spectra. Additionally, the linewidths for the Lorentzian signals are 306 (pristine) and 320 G (irradiated). The g-value found for the Lorentzian signal in both pristine and irradiated MST closely match values that have been previously reported for Mn^{2+} paramagnetic sites [26,27]. The Dysonian signal in the pristine MST spectra

was found to have a g-value of 1.9851 with a linewidth of 2609 G. From the irradiated MST spectra, the g-value was found to be 1.9682 along with linewidth of 2042 G. A significant decrease occurred after irradiation in the linewidth, which could indicate a change in the environment surrounding the paramagnetic signal reflected in the Dysonian signal. No additional signals from external impurities or irradiation were found indicating that proton irradiation did not form magnetically active defects in both MST crystals. This particular experiment confirms that Mn^{2+} (the only magnetically active ion in this compound) retained its valence state before and after proton irradiation. Thus, EPR spectra attests to the high quality of the MST crystals, which rule out the magnetic impurities other than Mn. These measurements lead to the belief that there may be significant changes on the valence state of non-magnetic element Te, which is associated with strong spin-orbit coupling that would alter the magnetic exchange interactions.

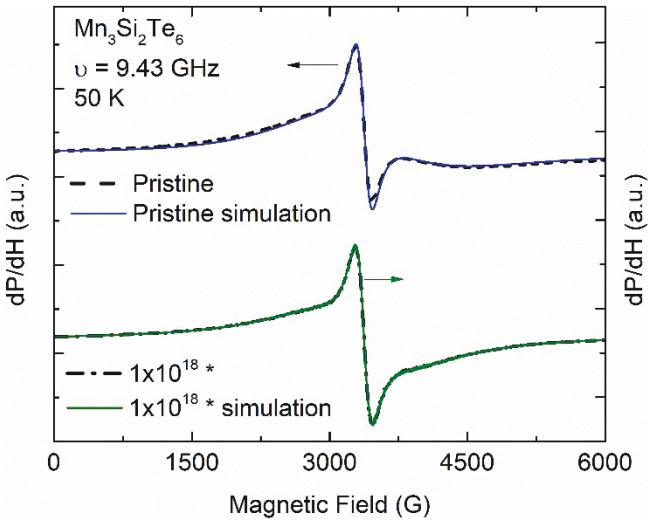

Figure 5. EPR spectra for pristine and irradiated MST measured at 50 K. (* represents the units of H^+/cm^2)

CONCLUSION

We have observed that the magnetization of ferrimagnetic vdW crystal MST is decreased upon proton irradiation. More strikingly, a decrease in the magnetization (49.2%) was observed upon proton irradiation as measured from the temperature dependent magnetization measurement performed in the H//*c* direction. We have studied the magneto-caloric effect and heat capacity upon proton irradiation and concluded that no significant change in the transition temperature occurred after proton irradiation. EPR spectra for pristine and irradiated MST revealed two overlapped signals originating from Mn^{2+}. Raman and XPS studies are under way to comprehend the changes observed in the magnetization of MST after irradiation. Scaling analysis of the magneto-caloric effect data for both crystals will be implemented as a next step. This work demonstrates that it is possible to modify the magnetic properties of magnetic vdW materials upon proton irradiation.

ACKNOWLEDGEMENTS

This work was prepared by C. L. Saiz, L. M. Martinez, A. Cosio, S. R. Singamaneni and co-authors under the award number 31310018M0019 from The University of Texas at El Paso (UTEP), Nuclear Regulatory Commission. The authors would like to acknowledge help received from J. H. Sohan in performing EPR measurements. The statements, findings, conclusions, and recommendations are those of the author(s) and do not necessarily reflect the view of UTEP or The Nuclear Regulatory Commission. C.L.S., A.C., and S. R. S. acknowledge support from the UTEP Start-up grant, as well as C. Petrovic and Y. Liu from Brookhaven National Laboratory for supplying all samples.

References

1 D. L. Duong, S. J. Yun, and Y. H. Lee, "van der Waals Layered Materials: Opportunities and Challenges," *ACS Nano*, vol. 11, no. 12, pp. 11803–11830, Dec. 2017.
2 P. Ajayan, P. Kim, and K. Banerjee, "Two-dimensional van der Waals materials," *Phys. Today*, vol. 69, no. 9, pp. 38–44, Aug. 2016.
3 C. Gong and X. Zhang, "Two-dimensional magnetic crystals and emergent heterostructure devices," *Science*, vol. 363, no. 6428, p. eaav4450, Feb. 2019.
4 Y. Liu, V. N. Ivanovski, and C. Petrovic, "Critical behavior of the van der Waals bonded ferromagnet $Fe_{3-x}GeTe_2$," *Phys. Rev. B*, vol. 96, no. 14, p. 144429, Oct. 2017.
5 B. Huang *et al.*, "Layer-dependent ferromagnetism in a van der Waals crystal down to the monolayer limit," *Nature*, vol. 546, no. 7657, pp. 270–273, Jun. 2017.
6 M. Bonilla *et al.*, "Strong room-temperature ferromagnetism in VSe 2 monolayers on van der Waals substrates," *Nat. Nanotechnol.*, vol. 13, no. 4, p. 289, Apr. 2018.
7 Z. Fei *et al.*, "Two-dimensional itinerant ferromagnetism in atomically thin Fe_3GeTe_2," *Nat. Mater.*, vol. 17, no. 9, p. 778, Sep. 2018.
8 M.-W. Lin *et al.*, "Ultrathin nanosheets of CrSiTe3: a semiconducting two-dimensional ferromagnetic material," *J. Mater. Chem. C*, vol. 4, no. 2, pp. 315–322, Dec. 2015.
9 A. F. May *et al.*, "Magnetic order and interactions in ferrimagnetic $Mn_3Si_2Te_6$," *Phys. Rev. B*, vol. 95, no. 17, p. 174440, May 2017.
10 Y. Liu and C. Petrovic, "Critical behavior and magnetocaloric effect in $Mn_3Si_2Te_6$," *Phys. Rev. B*, vol. 98, no. 6, p. 064423, Aug. 2018.
11 U. Abdurakhmanov, A. B. Granovskii, A. A. Radkovskaya, M. Kh. Usmanov, Sh. M. Sharipov, and V. P. Yugai, "The influence of neutron and proton irradiation on the magnetization of biotite," *Phys. Solid State*, vol. 44, no. 2, pp. 312–314, Feb. 2002.
12 S. W. Han *et al.*, "Controlling Ferromagnetic Easy Axis in a Layered MoS_2 Single Crystal," *Phys. Rev. Lett.*, vol. 110, no. 24, p. 247201, Jun. 2013.
13 L. Madauß *et al.*, "Defect engineering of single- and few-layer MoS_2 by swift heavy ion irradiation," *2D Mater.*, vol. 4, p. 015034, Mar. 2017.
14 P. Esquinazi, D. Spemann, R. Höhne, A. Setzer, K.-H. Han, and T. Butz, "Induced Magnetic Ordering by Proton Irradiation in Graphite," *Phys. Rev. Lett.*, vol. 91, no. 22, p. 227201, Nov. 2003.
15 K. W. Lee and C. E. Lee, "Electron Spin Resonance of Proton-Irradiated Graphite," *Phys. Rev. Lett.*, vol. 97, no. 13, p. 137206, Sep. 2006.
16 S. Mathew *et al.*, "Magnetism in MoS_2 induced by proton irradiation," *Appl. Phys. Lett.*, vol. 101, no. 10, p. 102103, Sep. 2012.
17 R.-W. Zhou *et al.*, "Ferromagnetism in proton irradiated 4H-SiC single crystal," *AIP Adv.*, vol. 5, no. 4, p. 047146, Apr. 2015.
18 R. C. Walker, T. Shi, E. C. Silva, I. Jovanovic, and J. A. Robinson, "Radiation effects on two-dimensional materials (Phys. Status Solidi A 12/2016)," *Phys. Status Solidi A*, vol. 213, no. 12, pp. 3268–3268, 2016.
19 A. V. Krasheninnikov and K. Nordlund, "Ion and electron irradiation-induced effects in nanostructured materials," *J. Appl. Phys.*, vol. 107, no. 7, p. 071301, Apr. 2010.
20 A. Geremew *et al.*, "Proton-Irradiation-Immune Electronics Implemented with Two-Dimensional Charge-Density-Wave Devices," *ArXiv190100551 Cond-Mat Physicsphysics*, Jan. 2019.
21 L. Shao *et al.*, "Standardization of accelerator irradiation procedures for simulation of neutron induced damage in reactor structural materials," *Nucl. Instrum. Methods Phys. Res. Sect. B Beam Interact. Mater. At.*, vol. 409, pp. 251–254, Oct. 2017.
22 J. G. Gigax, H. Kim, E. Aydogan, F. A. Garner, S. Maloy, and L. Shao, "Beam-contamination-induced compositional alteration and its neutron-atypical consequences in ion simulation of neutron-induced void swelling," *Mater. Res. Lett.*, vol. 5, no. 7, pp. 478–485, Nov. 2017.
23 J. P. Joshi and S. V. Bhat, "On the analysis of broad Dysonian electron paramagnetic resonance spectra," *J. Magn. Reson.*, vol. 168, no. 2, pp. 284–287, Jun. 2004.

24 C. P. Poole and H. A. Farach, “Line Shapes in Electron Spin Resonance,” p. 33.
25 C. P. J. Poole and H. A. Farach, *Handbook of Electron Spin Resonance*. Springer Science & Business Media, 1999.
26 P. A. Gonzalez Beermann, B. R. McGarvey, S. Muralidharan, and R. C. W. Sung, “EPR Spectra of Mn2+-Doped ZnS Quantum Dots,” *Chem. Mater.*, vol. 16, no. 5, pp. 915–918, Mar. 2004.
27 H. N. Ng and C. Calvo, “Crystal Structure of and Electron Paramagnetic Resonance of Mn2+ in Cd2(NH4)2(SO4)3,” *Can. J. Chem.*, vol. 53, no. 10, pp. 1449–1455, May 1975.